 CMES, vol.102, no.4, pp.331-343, 2014

Using Eulerlets to Give a Boundary Integral Formulation in Euler Flow and Discussion on Applications

Edmund Chadwick[1] **and Apostolis Kapoulas**

Abstract: Boundary element models in inviscid (Euler) flow dynamics for a manoeuvring body are difficult to formulate even for the steady case; Although the potential satisfies the Laplace equation, it has a jump discontinuity in two-dimensional flow relating to the point vortex solution (from the 2π jump in the polar angle), and a singular discontinuity region in three-dimensional flow relating to the trailing vortex wake. So, instead models are usually constructed bottom up from distributions of these fundamental solutions giving point vortex thin body methods in two-dimensional flow, and panel methods and vortex lattice methods in three-dimensional flow amongst others. Instead, the idea here is to present initially a boundary integral formulation in Euler flow that can then produce a true top down boundary element formulation. This is done for the steady two-dimensional case by matching the Euler flow to a far-field Oseen flow to determine the appropriate description for the Green's function Eulerlets. It is then shown how this reduces to the standard point vortex representations. Finally, two applications are outlined that can be used to test this approach, that of steady flow past a semi-infinite flat plate and steady flow past circular cylinder.

Keywords: Boundary Integral, Euler flow, Green's functions, Eulerlets, matched asymptotics.

1 Introduction

The classical methods for manoeuvring problems in inviscid flow theory (aeroplanes, ships, submarines, rockets) start by building up a solution for the velocity from a linear superposition of simple fundamental solutions, a bottom-up approach. For example, in slender body theory these are point sources [Thwaites, (1960)], in thin body (wing and aerofoil) theory these are point vortices in two-dimensional flow [Batchelor (1967)] and horseshoe vortices trailing into the wake forming a vortex lattice in three-dimensional flow [Lighthill (1986)]. They are positioned over

[1] University of Saford, Newton Building, Salford, UK. e.a.chadwick@salford.ac.uk

the body or on an inner camber line, and in the case of panel methods the velocity-discontinuous surface is continued into the wake [Katz and Plotkin (2001)]. Two important theoretical questions arise from these classical descriptions: why the particular choice of simple fundamental solution over other equally viable candidates, and why should a particular distribution of these presented in the description be used rather than any other equally possible descriptions? For example, in two-dimensional thin aerofoil theory, why should the point vortex fundamental solution be chosen over, say, the dipole whose potential is also single valued rather than multivalued, and why should an integral distribution of these over the camber line then describe the flow appropriately? It is clear that these are assumptions, see for example Batchelor (1967), so this is a theoretical problem needing to be addressed.

To do this, we provide a top-down approach by first giving a boundary integral description to the Euler equations in terms of Green's functions which we call Eulerlets. This is achieved by matching the far-field Oseen flow description to a near-field Euler flow description on a common matching boundary for large Reynolds number. As a first step, the small velocity perturbation Euler equations are considered. We present an argument for this procedure by drawing upon the similarity with the matching between far-field Oseen flow and near-field Stokes flow for small Reynolds number, see for example, Proudman and Pearson (1957), and Kaplun and Lagerstrom (1967). This fluid formulation can then be developed into a boundary element or meshless method, see for example Sellier (2013) and Langthjem and Nakano (2013). Once this is achieved, the resulting boundary integral formulation can then be approximated appropriately and discretized into a numerical scheme as required. Here, in particular we approximate the steady two-dimensional boundary integral description for small velocity perturbation Euler flow appropriately to obtain thin aerofoil theory and thin body theory. For future work, the small perturbation Euler flow will be further matched to an inner Euler flow creating three matching regions.

2 Matching procedure

We start with the far-field approximation to the flow given by the Oseen equations [Oseen (1927)] as

$$\rho U \frac{\partial u_i}{\partial x_1} = -\frac{\partial p}{\partial x_i} + \mu \frac{\partial^2 u_i}{\partial x_j \partial x_j}, \tag{1}$$

where x_i defines the Cartesian co-ordinate system using Einstein suffix notation, u_i is the velocity and p is the pressure. Oseen flow assumes a uniform flow field U in the x_1 direction. The fluid density is given by ρ, and viscosity given by μ.

By considering a dimensionless analysis, we then show how this gives a Stokes flow approximation in the near-field for low Reynolds number flow. This gives the standard description for low Reynolds number flow which matches a near-field Stokes flow to a far-field Oseen flow. Using the same arguments, we then go on to show how, again starting with the far-field Oseen flow approximation, we obtain the (small velocity perturbation) Euler flow approximation in the near-field for large Reynolds number flow. This gives our proposed description for large Reynolds number flow which matches a near-field Euler flow to a far-field Oseen flow.

Standard description for low Reynold number

The matching for low Reynolds number flow is well established [Proudman and Pearson (1957), and Kaplun and Lagerstrom (1957)] and can be viewed as a matching between a near-field Stokes flow and a far-field Oseen flow. Considering the dimensionless variables $x_j^* = x_j/l$, $u_i^* = u_i/U$ and the dimensionless Stokes pressure $p^* = p/(\mu U/l)$, eq (1) becomes

$$Re\frac{\partial u_i^*}{\partial x_1^*} = -\frac{\partial p^*}{\partial x_i^*} + \frac{\partial^2 u_i^*}{\partial x_j^* \partial x_j^*} \quad , \tag{2}$$

where l is the length dimension of the problem, U is a typical velocity and $Re = \rho U l/\mu$ is the Reynolds number. Neglecting the inertia term on the left hand side of eq (2) gives the Stokes flow equations. However, considering the far-field length L, then the inertia term can only be neglected if $Re\frac{L}{l}$ is small, otherwise the far-field Oseen equations given by eq (1) must be used instead of the near-field Stokes flow equations, see Fig. 1.

Proposed description for large Reynold number

We propose a matching for large Reynolds number flow viewed as a matching between a near-field Euler flow and a far-field Oseen flow. Now considering the dimensionless aerodynamic pressure $p^* = p/\left(\rho U^2\right)$, eq (1) becomes

$$\frac{\partial u_i^*}{\partial x_1^*} = -\frac{\partial p^*}{\partial x_i^*} + \frac{1}{Re}\frac{\partial^2 u_i^*}{\partial x_j^* \partial x_j^*} \quad . \tag{3}$$

For large Re, neglecting the viscous term on the far right hand side of eq (2) yields the (small velocity perturbation) frictionless ideal Euler equations. However, considering the far-field length L, the far-field Oseen wake is described by terms of the type $e^{-k(R-x_1)}$ in three-dimensions and of the type $e^{kx_1}K_0(kr)$ in two-dimensions, where $k = \rho U/2\mu$, R is the three-dimensional radius and r is the two-dimensional radius, see for example Chadwick (1998). Therefore diffusion of these wake terms

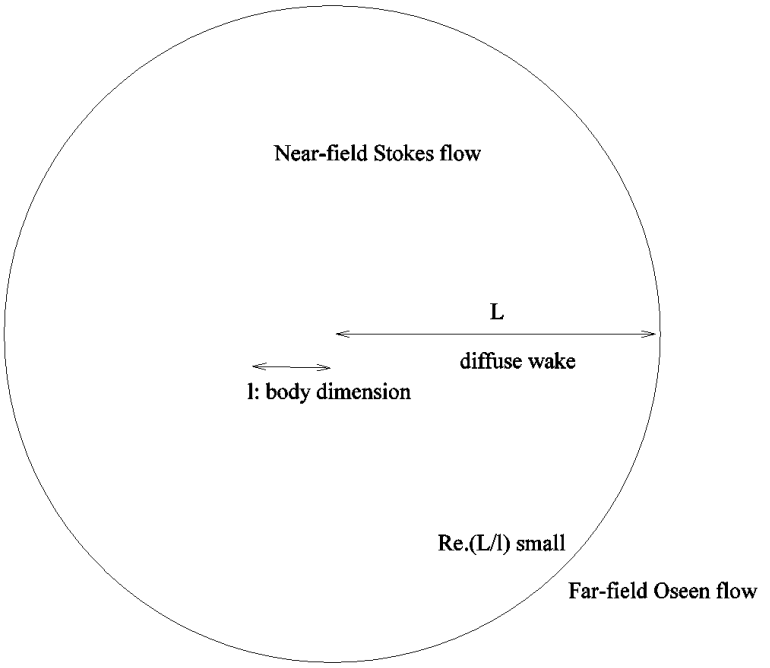

Figure 1: Matching regions for low Reynolds number flow.

is negligible if kl^2/L is large, which means $\frac{1}{Re}\frac{L}{l}$ is small. So in the near-field Euler flow approximation no wake diffusion is assumed, see Fig. 2.

3 Eulerlets

To find the Eulerlets that describe the near-field, again we follow a similar method as used by Chadwick (2013) to obtain near-field Stokelets by considering far-field Oseenlets. This method approximated the Oseenlets in the limit as $Re\frac{L}{l} \to 0$, and from this obtained the Stokeslets. Similarly, we will obtain the (small velocity perturbation) Eulerlets from the Oseenlets but this time consider the limit as $Re\frac{l}{L} \to \infty$ or equivalently $\frac{1}{Re}\frac{L}{l} \to 0$ instead.

The steady two-dimensional Oseenlets are [Oseen (1927), Chadwick (1998)]

$$u_i^{(1)} = \frac{1}{2\pi\rho U}\left[\frac{\partial}{\partial x_i}\left(\ln r + e^{kx_1}K_0(kr)\right) - 2ke^{kx_1}K_0(kr)\,\delta_{i1}\right],\ p^{(1)} = -\frac{1}{2\pi}\frac{\partial}{\partial x_1}\ln r,$$

$$u_i^{(2)} = \frac{1}{2\pi\rho U}\varepsilon_{ij3}\frac{\partial}{\partial x_j}\left(\ln r + e^{kx_1}K_0(kr)\right),\ p^{(2)} = -\frac{1}{2\pi}\frac{\partial}{\partial x_2}\ln r, \tag{4}$$

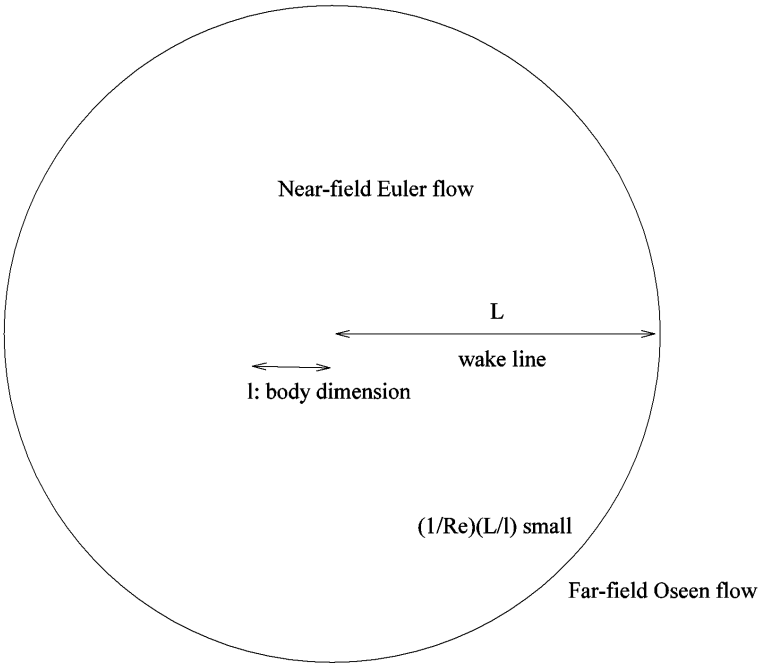

Figure 2: Matching regions for large Reynolds number flow.

where the Green's functions for Oseen flow with uppercase suffix (1) denotes the unit drag Oseenlet and with suffix (2) denotes the unit lift Oseenlet. The symbol δ_{ij} is Kronecker delta where $\delta_{ij} = 1$ when $i = j$ and is zero otherwise. The symbol ε_{ijk} is 1 when i, j, k are in ascending wrapped order, -1 in descending wrapped order, and zero otherwise. Let us now investigate these Oseenlets in the limit as $Re\frac{l}{L} \to \infty$. We have $e^{kx_1}K_0(kr) \to \sqrt{\frac{\pi}{2kr}}e^{-kx_2^2/2x_1}$. In order for the boundary integral formulation to be consistent, the boundary integrals evaluated from the Oseenlets must give the same values as the boundary integral evaluations from the Eulerlets. This means that the evaluations from integral wake cross-sections must match on the common boundary. Let us investigate these integral wake cross-sections by considering $\int_{-\infty}^{\infty} e^{kx_1}K_0(kr)\,dx_2$. Letting $= \sqrt{\frac{k}{2x_1}}x_2$, and noting that $r \approx x_1$, then

$$\int_{-\infty}^{\infty} e^{kx_1}K_0(kr)\,dx_2 = \int_{-\infty}^{\infty} \frac{\sqrt{\pi}}{k}e^{-\eta^2}d\eta = \frac{\pi}{k}. \tag{5}$$

Noting that derivatives are given by $\frac{\partial}{\partial x_1} = -\frac{\eta}{2x_1}\frac{\partial}{\partial \eta}$ and $\frac{\partial}{\partial x_2} = \sqrt{\frac{k}{2x_1}}\frac{\partial}{\partial \eta}$, then in the limit integral cross-sections of the derivatives of the integrand given in eq (5) will be

zero. This means that, of the wake terms in eq (4), only the wake cross section from the term $2ke^{kx_1}K_0(kr)\delta_{i1}$ in the drag Oseenlet gives a non-zero contribution, and so in the limit all the other wake terms disappear. In this limit, the wake collapses onto the wake half line $x_1 > 0, x_2 = 0$. So in the limit eq (5) becomes

$$\int_{-\infty}^{\infty} e^{kx_1}K_0(kr)\,dx_2 = \frac{\pi}{k}\int_{-\infty}^{\infty} H(x_1)\,\delta(x_2)\,dx_2 = \frac{\pi}{k}, \tag{6}$$

where $\delta(x_2)$ is the Dirac delta function such that $\delta(x_2) = 0$ for $x_2 \neq 0$, and the integration across $x_2 = 0$ gives, for example, $\int_{-\infty}^{\infty} \delta(x_2)\,dx_2 = 1$; and $H(x_1)$ is the Heaviside function $H(x_1) = 0$ for $x_1 < 0$, $H(x_1) = 1$ for $x_1 > 0$, and at $x_1 = 0$ we have $\frac{\partial}{\partial x_1}H(x_1) = \delta(x_1)$. The Oseenlets given by eq (4) therefore reduce to the Eulerlets

$$u_i^{(1)} = \frac{1}{2\pi\rho U}\left[\frac{\partial}{\partial x_i}(\ln r) - 2\pi H(x_1)\,\delta(x_2)\,\delta_{i1}\right],\ p^{(1)} = -\frac{1}{2\pi}\frac{\partial}{\partial x_1}\ln r,$$

$$u_i^{(2)} = \frac{1}{2\pi\rho U}\varepsilon_{ij3}\frac{\partial}{\partial x_j}(\ln r),\ \ p^{(2)} = -\frac{1}{2\pi}\frac{\partial}{\partial x_2}\ln r, \tag{7}$$

in the limit. So the drag Eulerlet is a potential source outflow with an equal inflow along the wake half line, see Fig. 3, and the lift Eulerlet is a clockwise point vortex, see Fig. 4. We note that Batchelor (1967) presents a sketch similar to Fig. 3 to represent the inflow due to the drag of a body. However, he does not associate it with the drag Eulerlet, or attempt to describe it mathematically. Also, we note that in thin aerofoil theory [Batchelor (1967), Katz and Plotkin (2001)] a distribution of point vortices along the camber line are assumed, producing lift.

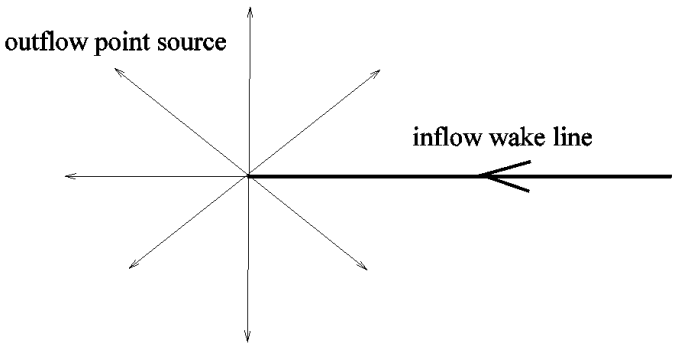

Figure 3: Drag Eulerlet.

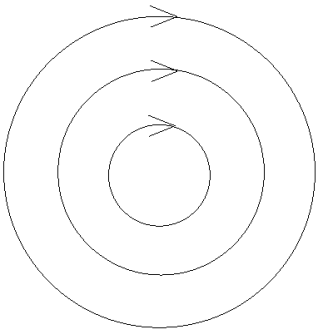

Figure 4: Lift Eulerlet.

It remains to ask whether these satisfy the (small velocity perturbation Euler equations) for the Eulerlets given by

$$\rho U \frac{\partial u_i^{(m)}}{\partial x_1} = -\frac{\partial p^{(m)}}{\partial x_i} - f_i^{(m)} \tag{8}$$

where $f_i^{(m)} = \delta(x_1)\,\delta(x_2)\,\delta_{im}$, the function $\delta(.)$ being the Dirac delta function and the symbol δ_{ij} being Kronecker delta. For the drag Eulerlet, $\rho U \frac{\partial u_i^{(1)}}{\partial x_1} = \frac{1}{2\pi}\frac{\partial}{\partial x_1}\left(\frac{\partial}{\partial x_i}\ln r - 2\pi H(x_1)\,\delta(x_2)\,\delta_{i1}\right) = \frac{1}{2\pi}\frac{\partial}{\partial x_1}\left(\frac{\partial}{\partial x_i}\ln r) - \delta(x_1)\,\delta(x_2)\,\delta_{i1}\right) = -\frac{\partial p^{(1)}}{\partial x_i} - f_i^{(1)}$, and so satisfies eq (8). For the lift Eulerlet, $\rho U \frac{\partial u_i^{(2)}}{\partial x_1} = \frac{1}{2\pi}\frac{\partial}{\partial x_1}\left(\varepsilon_{ij3}\frac{\partial}{\partial x_j}\ln r\right)$. For $i=1$, this gives $\frac{1}{2\pi}\frac{\partial}{\partial x_1}\left(\frac{\partial}{\partial x_2}\ln r\right) = -\frac{\partial p^{(2)}}{\partial x_1}$, and for $i=2$ this gives $-\frac{1}{2\pi}\frac{\partial^2}{\partial x_1^2}\ln r = \frac{1}{2\pi}\frac{\partial^2}{\partial x_2^2}\ln r - \delta(x_1)\,\delta(x_2) = -\frac{\partial p^{(2)}}{\partial x_2} - f_2^{(2)}$, and so also satisfies eq (8).

4 Green's integral representation.

Near-field

We follow the same Green's integral derivation as given by Chadwick (2013), which is itself equivalent to the procedure outlined by Oseen (1927). Consider the (small velocity perturbation) Euler equations that hold in the near-field and given by

$$\rho U \frac{\partial u_i}{\partial y_1} = -\frac{\partial p}{\partial y_i} - f_i \tag{9}$$

where f_i represents an external force applied on the fluid, so in a fluid region away from a boundary and free from external body force fields, this is zero, and we have used a new Cartesian co-ordinate system y_i which in the Green's integral representation will represent points integrated over in the Green's integral expression. So this is different from the original Cartesian co-ordinate system x_i which represents a point in the fluid. For brevity, let us also define a third Cartesian co-ordinate $z_i = x_i - y_i$ which links the two. So, if an integral distribution of Green's functions are positioned over the space parameterized by y_i , then the vector distance from the point in the fluid x_i to the Green's function origin at y_i is given by z_i. Following the Green's integral derivation, then let us consider

$$\int_{\sum}\left[\left(\frac{\partial p(\boldsymbol{y})}{\partial y_i}+\rho U\frac{\partial u_i(\boldsymbol{y})}{\partial y_1}+f_i(\boldsymbol{y})\right)u_i^{(m)}(\boldsymbol{z})-\left(\frac{\partial p^{(m)}(\boldsymbol{z})}{\partial z_i}+\rho U\frac{\partial u_i^{(m)}(\boldsymbol{z})}{\partial z_1}+f_i^{(m)}(\boldsymbol{z})\right)u_i(\boldsymbol{y})\right]d\sum$$

which is identically zero from eq (8) and eq (9). Noting that $\frac{\partial}{\partial z_i}=-\frac{\partial}{\partial y_i}$ this gives

$$\int_{\sum}\left[\left(\frac{\partial p(\boldsymbol{y})}{\partial y_i}+\rho U\frac{\partial u_i(\boldsymbol{y})}{\partial y_1}+f_i(\boldsymbol{y})\right)u_i^{(m)}(\boldsymbol{z})-\left(-\frac{\partial p^{(m)}(\boldsymbol{z})}{\partial y_i}-\rho U\frac{\partial u_i^{(m)}(\boldsymbol{z})}{\partial y_1}+f_i^{(m)}(\boldsymbol{z})\right)u_i(\boldsymbol{y})\right]d\sum=0$$

and after rearrangement to prepare for application of the divergence theorem we get

$$\begin{aligned}&\int_{\sum}\left[\frac{\partial}{\partial y_i}\left(p(\boldsymbol{y})u_i^{(m)}(\boldsymbol{z})\right)+\frac{\partial}{\partial y_i}\left(p^{(m)}(\boldsymbol{z})u_i(\boldsymbol{y})\right)+\rho U\frac{\partial}{\partial y_1}\left(u_i(\boldsymbol{y})u_i^{(m)}(\boldsymbol{z})\right)\right.\\&\left.+f_i(\boldsymbol{y})u_i^{(m)}(\boldsymbol{z})-f_i^{(m)}(\boldsymbol{z})u_i(\boldsymbol{y})\right]d\sum=0\end{aligned}$$

Assuming that $\sum$ represents a contiguous space bounded by a surface (curve in two-dimensions) $\partial\sum$ which has defined an outward pointing normal $n_i^{\sum}$ to the space $\sum$, then applying the divergence theorem we get

$$\int_{\partial\sum}[p(\boldsymbol{y})u_i^{(m)}(\boldsymbol{z})n_i\sum+p^{(m)}(\boldsymbol{z})u_i(\boldsymbol{y})n_i\sum+\rho U u_i(\boldsymbol{y})u_i(m)(\boldsymbol{z})n_i\sum]d\partial\sum=u_i(\boldsymbol{x})\delta_{im}$$

where we have assumed that $f_i = 0$ in the fluid region $\sum$. Consider the fluid region $\sum$ bounded by the curve C that encloses the body or fluid disturbance in the near-field, and the curve C_{match} that is in the matching region between the Oseen and Euler flow fields, see Fig. 5.

Far-field

The boundary integral over C_{match} matches to first order an Oseen flow boundary integral. This integral can then be taken as far away as desired in the far-field Oseen flow region, and for this formulation it is shown that this integral is zero by Fishwick and Chadwick (2006).

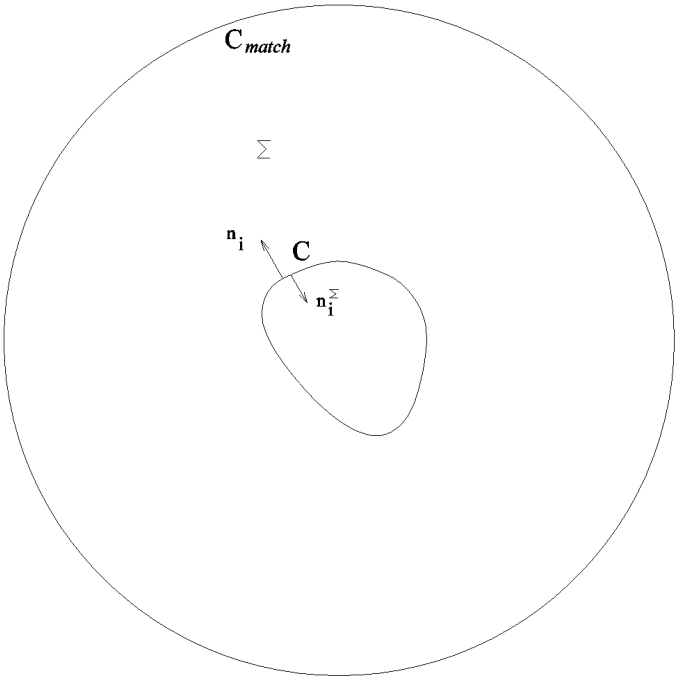

Figure 5: The near-field boundary integral.

5 Boundary integral formulation in Euler flow

Giving the representation in terms of the outward pointing normal n_i to C, where on C we have that $n_i = -n_i^{\Sigma}$, and the integration over C_{match} is taken to be zero, gives a boundary integral formulation in Euler flow

$$u_m = -\int_C \left(p(\boldsymbol{y})\, u_i^{(m)}(\boldsymbol{z})\, n_i + p^{(m)}(\boldsymbol{z})\, u_i(\boldsymbol{y})\, n_i + \rho U u_i(\boldsymbol{y})\, u_i^{(m)}(\boldsymbol{z})\, n_1 \right) dl. \tag{10}$$

Noting that $u_i^{(m)} = u_m^{(i)}$ and letting $\phi^{(1)} = \frac{1}{2\pi\rho U} \ln r$, $\phi^{(2)} = -\frac{1}{2\pi\rho U}\theta$, where θ is the polar angle, then eq (10) becomes

$$u_m = -\int_C \left(p(\boldsymbol{y})\, u_m^{(i)}(\boldsymbol{z})\, n_i - \rho U \phi^{(1)}(\boldsymbol{z})_{,m}\, u_i(\boldsymbol{y})\, n_i + \rho U u_i(\boldsymbol{y})\, u_m^{(i)}(\boldsymbol{z})\, n_1 \right) dl \quad ,$$

where we have used the notation $\phi^{(1)}(\boldsymbol{z})_{,m} = \frac{\partial \phi^{(i)}(z)}{\partial z_m}$. So we can express the velocity as a potential velocity part plus a wake velocity part $u_m = \phi_{,m} + w_m$, noting that the potential is then described in terms of an integral distribution of point vortices for which the polar angle is 2π discontinuous for a revolution around each vortex

point. This potential is given by

$$\phi = -\int_C \left(p(\boldsymbol{y})\,\phi^{(i)}(\boldsymbol{z})\,n_i - \rho U \phi^{(1)}(\boldsymbol{z})\,_{,m} u_i(\boldsymbol{y})\,n_i + \rho U u_i(\boldsymbol{y})\,\phi^{(i)}(\boldsymbol{z})\,n_1 \right) dl \tag{11}$$

and the wake velocity by $w_m = -\int_C \left(p(\boldsymbol{y})\,w_m^{(1)}(\boldsymbol{z})\,n_1 + \rho U u_1(\boldsymbol{y})\,w_m^{(1)}(\boldsymbol{z})\,n_1 \right) dl$, where $w_m^{(1)} = -\frac{1}{\rho U} H(x_1)\,\delta(x_2)\,\delta_{m1}$. So $w_2 = 0$ and

$$w_1 = -\int_C \rho U w_1(\boldsymbol{y})\,w_1^{(1)}(\boldsymbol{z})\,n_1 dl = \int_C w_1(\boldsymbol{y})\,H(x_1)\,\delta(x_2)\,n_1 dl \quad . \tag{12}$$

6 Thin aerofoil and thin body theory

We can now show how this formulation reduces to standard theories. For thin aerofoil theory, let us invoke the Kutta condition, and so assume a wake line that emerges at the trailing edge, see Fig. 6.

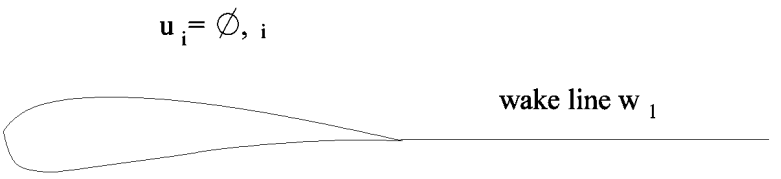

Figure 6: Kutta condition for thin aerofoil theory.

Then the boundary condition is satisfied by the potential only, and so eq (11) becomes

$$\phi = -\int_C \left(p\varphi^{(1)} n_1 + p\varphi^{(2)} n_2 - \rho U \varphi^{(1)} u_1 n_1 - \rho U \varphi^{(1)} u_2 n_2 + \rho U u_1 \phi^{(1)} n_1 + \rho U u_2 \phi^{(2)} n_1 \right) dl. \tag{13}$$

However, we have that $p = -\rho U \varphi_{,1}$ and over the boundary, $u_i = \phi_{,i}$. So eq (13) becomes after some cancellation

$$\begin{aligned} \phi &= \rho U \int_C \left(\phi_{,1} n_1 + \phi_{,2} n_2\right) \phi^{(1)} + \left(\phi_{,1} n_2 - \phi_{,2} n_1\right) \phi^{(2)} dl \\ &= \frac{1}{2\pi} \int_C \left\{ (\nabla\phi . \boldsymbol{n}) \ln r + (\nabla\phi \times \boldsymbol{n})_3 (-\theta) \right\} dl \end{aligned} \tag{14}$$

where $\boldsymbol{n} = (\boldsymbol{n}_1, \boldsymbol{n}_2)$. The term $\boldsymbol{s} = \boldsymbol{\nabla\phi}.\ \boldsymbol{n}$ represents the outflow strength of the distribution of sources, and the term $\boldsymbol{\gamma} = \boldsymbol{\nabla\phi} \times \boldsymbol{n}$ represents the clockwise circulation

strength of the distribution of clockwise point vortices. So we can split the potential in eq (14) into $\boldsymbol{\phi} = \boldsymbol{\phi}^D + \boldsymbol{\phi}^L$ such that

$$\phi^D = \frac{1}{2\pi} \int_C s(l) \ln r dl$$

represents a distribution of point sources. Over an internal line axis, this gives the thin body (or two –dimensional slender body) theory. This also means

$$\phi^L = \frac{1}{2\pi} \int_C \gamma(l)(-\theta) dl$$

which represents a distribution of point vortices. Over an internal axis, this gives thin aerofoil theory.

7 Applications

Two applications are outlined that can be used to test this approach, that of steady flow past a semi-infinite flat plate and steady flow past a circular cylinder.

7.1 Steady flow past a semi-infinite flat plate

This problem is given by the Blasius equation and similarity solution, and generalized by the Faulkner-Skan equations for flow past a semi-infinite wedge. Let us consider modeling this problem in a different way, by considering three regions in Stokes flow, Oseen flow and Euler flow, and match using the boundary integral formulation given above, see Figure 7. This will provide a test for the formulation, and also open the possibility of modeling more general shapes using a boundary element solver where the similarilty solution cannot be used.

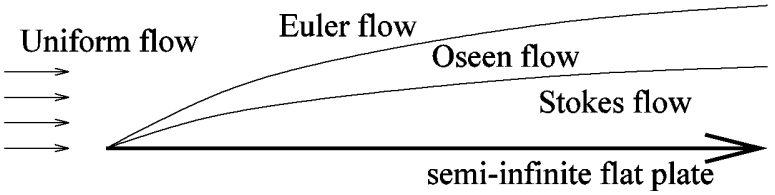

Figure 7: Steady flow past a semi-finite flate plate.

7.2 Steady flow past a circular cylinder

Other problems that can use Eulerlets are those with bluff bodies, for example circular cylinders. In this problem, the far-field profile will be a given, and from

this a drag Eulerlet distribution formulated. This problem is particularly interesting because this Eulerlet representation predicts drag, which is not possible for standard Euler models because of D'Alembert's paradox. However, the additional terms in the new Eulerlet formulation provide a drag inflow, which is balanced by a potential outflow giving drag. Hence, a particular test for the formulation is the closeness to the drag value for flow past a circular cylinder with a given far-field profile, see Figure 8.

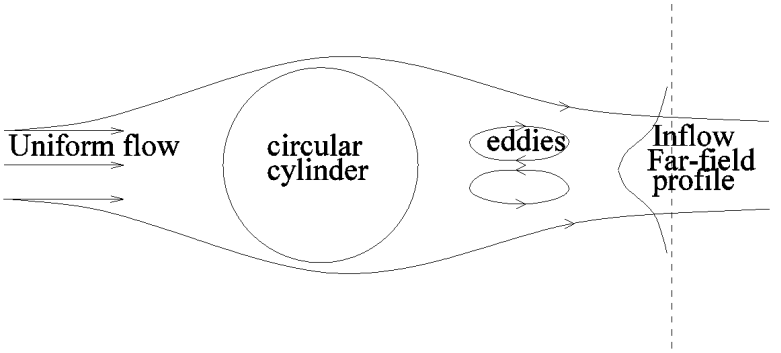

Figure 8: Steady flow past a circular cylinder.

8 Summary

We have obtained a boundary integral formulation in steady two-dimensional Euler flow from a matching between near-field Euler flow and far-field Oseen flow. We have further demonstrated that this formulation reduces to thin body and thin aerofoil theory. In the matching, a wake inflow term must be retained and is present in the description of the drag Eulerlet. The other term in the drag Eulerlet is the potential outflow term, and the lift Eulerlet is represented by a clockwise point vortex. We outline two test problems for the method, that of steady flow past a flat plate and uniform flow past a circular cylinder. The next step is to develop a code using Boundary Element Eulerlets, and investigate the accuracy in relation to these two problems. If the tests prove successful, then the code can be developed to tackle more complex shapes.

References

Batchelor, G. K. (1967): *An introduction to fluid dynamics*, Cambridge University Press.

Chadwick, E. (1998): The far-field Oseen velocity expansion. *Proc. R. Soc. A.*, vol. 454, no. 1976, pp. 2059-2082.

Chadwick, E. A. (2013): The far-field Green's integral in Stokes flow from the boundary integral formulation, *Comp. Mod. Engng. Sci. (CMES)* **96** no. 3 177-184.

Fishwick, N.; Chadwick, E. (2006): The evaluation of the far-field integral in the Green's function representation for steady Oseen flowGreen's integral in Stokes flow from the boundary integral formulation. *Phys. Fluid*, vol. 18, issue 11, pp. 113101-5.

Kaplun, S.; Lagerstrom, P. A. (1957): Asymptotic expansions of Navier-Stokes solutions for small Reynolds numbers. *J. Math. Mech.*, vol. 6 , pp. 595-603.

Katz, J.; Plotkin, A. (2001): *Low speed aerodynamics, 2nd edition,* Cambridge University Press.

Langthjem, M. A.; Nakano, M. (2013): Application of the time-domain boundary element method to analysis of flow-acoustic interaction in a hole-tone feedback system with a tailpipe. *Comp. Mod. Engng. Sci. (CMES)*, vol. 96 , no. 4, pp. 227-241.

Lighthill, M. J. (1986): *An informal introduction to theoretical fluid mechanics*, Clarendon Press.

Oseen, C. W. (1927): *Neuere Methoden und Ergebnisse in der Hydrodynamik,* in Akad, Verlagsgesellschaft, Leipzig.

Proudman, I.; Pearson, J. R. A. (1957): Expansions at small Reynolds numbers for the flow past a sphere and a circular cylinder. *J. Fluid Mech.*, vol. 2 , no. 3, pp. 237-265.

Sellier, A. (2013): Arbirary Stokes flow about a fixed or freely suspended Stokes particle. *Comp. Mod. Engng. Sci. (CMES)*, vol. 96 , no. 3, pp. 159-176.

Thwaites, B. (1960): (ed.) *Incompressible Aerodynamics*, Dover.